European Journal of Applied Sciences – Vol. 13, No. 02
Publication Date: April 25, 2025
DOI:10.14738/aivp.1302.18168.
Hosino, M. (2025). Nematic Phase Transitions in an Assembly of Molecules with a Bent Core. European Journal of Applied Sciences, Vol - 13(02). 153-164.

Nematic Phase Transitions in an Assembly of Molecules with a Bent Core

Masahito Hosino
Independent researcher, Norikura 1-1303-2,
Midori-ku, Nagoya 458-0004, Japan

ABSTRACT

Approximately 20 years ago, Hosino and Nakano [1] investigated the phase transitions in an assembly of biaxial molecules that interact via dispersion forces, discovering the existence of one uniaxial and two biaxial nematic phases and disconematic phase in the assembly. Follow-up studies obtained valuable results on the phase transitions in an assembly of biaxial molecules with hard cores [2], chirality [3, 4], and flexibility [5] based on the initially proposed method [1]. In this study, the phase transitions in the assembly of molecules with a bent core were investigated using the same method, demonstrating the occurrence of sequence of transitions between various nematic phases in the system.

Keyword: bent-core molecules, temperature dependence of anisotropic parameters, sequence of transitions between nematic phases

INTRODUCTION

Approximately 20 years ago, Hosino and Nakano [1] investigated the phase transitions in an assembly of biaxial molecules that interact via dispersion forces, thereby noting the existence of a uniaxial and two biaxial nematic phases and a disconematic phase.

In addition, the phase diagram revealed sequence of transitions between these phases at points where anisotropy parameters ε_x and ε_y, which represent the anisotropy in the x and y directions of a molecule toward the z direction, respectively, are limited. As such, subsequent studies proposed the use of the initially proposed the analytical method [1] to investigate the phase transitions in an assembly of biaxial molecules with hard cores [2], and a system of molecules with a chiral plane [3, 4]. These investigations revealed the similar phase transition diagrams in a system of molecules with hard cores and molecules interacting via dispersion forces. In addition, the mechanism for the chiral phases in a molecular system with chiral plane was elucidated. Recently, the method obtained by Hosino and Nakano [1] was used to analyze the phase transitions in an assembly of flexible molecules [5]. Thus, the proposed analytical method was demonstrated to be a useful and powerful tool for investigating biaxial liquid crystals.

Several experimental and theoretical works have focused on bent liquid crystalline molecules over the past decades [6]. It is noticed that there are two types in regard of bent liquid crystalline molecule. One is a molecule having a bent core with a wing at each side of its core. Another one is dimers linked by flexible chain. Both types of molecule bend depending on temperature and/or a density of molecules. However, different model has to be proposed for each type of molecule, respectively. The molecular model of dimers linked by flexible chain was already proposed and the dependence of nematic transitions on molecular shape and/or

anisotropy of interaction was elucidated [7, 8]. In those studies, the dependence of molecular shape and/or anisotropy of interaction on temperature is induced by the internal rotation around the C—C bond in the alkyl chain when transforming between the gauche and trans states [9, 10]. However, another type bent liquid crystalline molecule can't give rise to such an internal rotation as dimers linked by flexible chain. So then, molecular model of biaxial molecule with bent core, which has a mechanism giving the dependence of molecular shape and/or anisotropy of interaction on temperature, is proposed in present study. Molecular model in present study can be expanded to the one of dimers linked by flexible chain, and such an expanded model elucidates nematic transitions more clearly than the studies carried out until now, because the dependence of anisotropy parameters εx and εy on temperature can be obtained accurately, and the proposed method described in previous work [5] elucidates more clearly nematic transitions basing on phase diagram on these anisotropy parameters plane. Furthermore, in such an expanded model, molecular shapes including chiral one are explicitly defined depending on temperature. This fact is very important to elucidate phase transitions among various smectic phases as SmA, SmC, and SmC* phases. The interaction potential between a pair of molecules based on previously developed analytical methods [1—5] and one of a system of biaxial molecules with a bent core were similar, whereby, εx and εy are functions of θ_B as follows:

$$\varepsilon_x = cos(\theta_B/2)/sin(\theta_B/2)\ ,\ \varepsilon_y = 0. \tag{1}$$

As the dependence of θ_B on the temperature could be estimated, (as described in Section 2), the previously proposed approach [5] elucidated the phase transition of the assembly of molecules with a bent core.

INTRAMOLECULAR INTERACTION AND DEPENDENCE OF θ_B ON TEMPERATURE

As an example, the molecule of the mesogenic compound 4,6-dichloro-1,3-phenylene bis [4- (4-n-alkyloxy-3-fluoro-phenyliminomethyl) benzoate] [Fig.1(a) and 1(b)] was considered to be a biaxial molecule with a bent core. The θ_B value of this molecule was limited to the range of $2\pi/3$ to π. The upper limit of θ_B was attributed to the repulsion force between the chlorine substituent on the phenylene group and oxygen atom of carboxyl group, whereas lower limit of θ_B, was ascribed the structure of the phenylene group. In addition, dipoles induced in the benzoate groups of either side of the molecular core and both intra-molecular and inter-molecular interactions were induced between the pairs of induced dipoles. The sides of the molecule are denoted as sides A and B (Fig. 1(b)).

With respect to the intramolecular interaction, the pseudopotential for limiting θ_B is introduced as

$$U_{pseu}(cos\theta_B) = \frac{U_{pseu}^{Cl}}{cos\,(\theta_B)+1} - \frac{U_{pseu}^{0}}{cos\,(\theta_B)+1/2} \tag{2}$$

Although other functions of $\cos(\theta_B)$ can be introduced as the pseudopotential for the limiting on θ_B, Eq. (2) was conveniently adopted in this work. The intramolecular interaction caused by the induced dipoles at both sides of the core is

$$U_{dis}(cos\theta_B) = -\frac{U^0_{dis}}{|\overrightarrow{r_{AB}}|^{2n}}(cos\theta_B)^2 = -\frac{U^0_{dis}}{(2r_0)^{2n}}\frac{(cos\theta_B)^2}{\left(sin(\theta_B/2)\right)^{2n}} = -\frac{U^0_{dis}}{(2r_0)^{2n}}\frac{(cos\theta_B)^2}{(1-cos\theta_B)^n} \quad (3)$$

where $\overrightarrow{r_{AB}}$ is the distance between the induced dipoles on sides A and B and r0 is the distance between the center of the molecule and point at which the dipole was induced. Eq. (3) was introduced as an application of Eq. (9) in Ref. [1].

The average of quantities Q depending on $cos\theta_B$ is

$$\langle Q(cos\theta_B)\rangle_{cos\theta_B} = \frac{\int Q(cos\theta_B)P(cos\theta_B)d(cos\theta_B)}{\int P(cos\theta_B)d(cos\theta_B)} \quad (4)$$

where $P(cos\theta_B)$ is a weight function with respect to $cos\theta_B$, calculated as

$$P(cos\theta_B) = P_0 exp\left(-\frac{U_{pseu}(cos\theta_B)}{\overline{U^0_{dis}}} - \beta U_{dis}(cos\theta_B)\right). \quad (5)$$

In Eq. (5), $U_{pseu}(cos\theta_B)$ is normalized with $\overline{U^0_{dis}} \equiv U^0_{dis}/(2r_0)^{2n}$, instead of kBT, because it is largely independent of the temperature and imposes the limitation on cosθB. Meanwhile, $U_{dis}(cos\theta_B)$ was normalized with kBT because the interaction represented with this potential highly depends on the temperature. Although the average cosθB, denoted as $cos\theta_B^{av}$, could be obtained using Eq. (4), such a calculation is difficult. Therefore, a simpler method was proposed to obtain $cos\theta_B^{av}$. As P(cosθB) reaches its maximum value at $cos\theta_B^{av}$, $\partial P(cos\theta_B)/\partial(cos\theta_B) = 0$:thus, following equation is deduced as

$$-\frac{U^{Cl}_{pseu}/\overline{U^0_{dis}}}{\left(cos\theta_B^{av}+1\right)^2} + \frac{U^{O}_{pseu}/\overline{U^0_{dis}}}{\left(cos\theta_B^{av}+1/2\right)^2} = \frac{2\overline{U^0_{dis}}}{k_BT}\frac{2cos\theta_B^{av}+(2+n)\left(cos\theta_B^{av}\right)^2}{\left(1-cos\theta_B^{av}\right)^{n+1}}. \quad (6)$$

Eq. (6) can be solved graphically as shown in Fig. 2(a). First, curve lL was drawn by plotting the values on the left-hand sides of Eq. (6) on the x − y plane for each of cosθB value. lL was drawn within the cosθB range from $-1/2$ to -1. Similarly, lR was drawn by plotting the values of the right-hand side of Eq. (6) on the same plane for each cosθB value.

The solution of Eq. (6) is given as the intersection of lL and lR. lL intersects the x-axis at $cos\theta_B^0$ where the value of the pseudopotential is minimized. Moreover, the curve lL becomes infinitely monotonic and asymptotic near $cos\theta_B = -1/2$ as $cos\theta_B$ increases from $cos\theta_B^0$ to $-1/2$. As cosθB decreases from $cos\theta_B^0$ to -1, lL becomes infinitely monotonic and asymptotic near $cos\theta_B = -1$. In contrast, lR intersects the x-axis at cosθB = 0 and − 2/(n+2), which remains below the x-axis in the cosθB region from 0 to − 2/(n+2). Above the x-axis, lR exists as an approximately straight line. When cosθB $\langle$ − 2/(n+2), lR has a slightly upward convex. Hereafter, n=3, in which − 2/(2+n) is equal to − 0.4, was assumed. When the temperature decreased to 0, lR became asymptotic to the cosθB = − 0.4. when the temperature increased from 0 to infinity, lR became asymptotic to the x-axis.

Therefore, an intersection always exists between the curves for all temperatures. As the temperature decreased to 0, $\cos\theta^B$ increased to $-1/2$ and ε_x increased to $\frac{\sqrt{3}}{3} \approx 0.5774$. As the temperature increased from 0 to infinity, $\cos\theta_B$ decreased to $cos\theta_B^0$ and ε_x decreased to ε_x^0, as defined in

$$\varepsilon_x^0 = \sqrt{(1 + cos\theta_B^0)/(1 - cos\theta_B^0)}\,. \tag{7}$$

Using parameter u defined as $\left(U_{pseu}^{Cl}/U_{pseu}^{O}\right)^{\frac{1}{2}}$, $cos\theta_B^0$ and ε_x^0 are expressed as

$$cos\theta_B^0 = -\frac{1}{2} \bullet \frac{u+2}{u+1}, \tag{8}$$

$$\varepsilon_x^0 = \left(\frac{1-1/(1+u)}{3+1/(1+u)}\right)^{\frac{1}{2}}. \tag{9}$$

Overall, ε_x decreases from 0.5574 to ε_x^0, as the temperature increases from 0 to infinity, determining the dependence of ε_x on temperature. Interestingly, the dependency of ε_x on temperature depends on u, which represents the intramolecular interactions as U_{pseu}^{Cl} and U_{pseu}^{O} [Fig. 2(b)]. The dependence of ε_x on $\bar{T}$ is depicted in $\varepsilon_x(\bar{T}: \varepsilon_x^0)$ curve, where $\bar{T}$ is the normalized temperature $\bar{T} = k_B T/2\overline{U_{dis}^0}$. These results of the dependence of θ_B on temperature derived in this section are the reasonable and consistent with the experimental results [10]. The results obtained in this section are discussed in Section 3.

INTERMOLECULAR INTERACTION

Subsequently, the intermolecular interaction potential between the I- and J-th molecules was investigated, as follows:

$$\Phi_{IJ}(R_{IJ}) = \Phi(\vec{p}_A(I), \vec{p}_A(J)) + \Phi(\vec{p}_A(I), \vec{p}_B(J)) + \Phi(\vec{p}_B(I), \vec{p}_A(J)) + \Phi(\vec{p}_B(I), \vec{p}_B(J)) \tag{10}$$

where $\vec{p}_A(I)$ is the dipole induced in the group on A side of the I-th molecule, and $\Phi(\vec{p}_A(I), \vec{p}_A(J))$ is the potential of the interaction between $\vec{p}_A(I)$ and $\vec{p}_A(J)$. $\vec{p}_A(I)$ and $\vec{p}_B(I)$ are expressed in the molecular coordinate system as $(|\vec{p}_A(I)|cos(\theta_B/2), 0, |\vec{p}_A(I)|sin(\theta_B/2))$ and $(|\vec{p}_B(I)|cos(\theta_B/2), 0, -|\vec{p}_B(I)|sin(\theta_B/2))$, respectively. The direction of the long axis of the molecule and direction of vector $\overrightarrow{r_A} + \overrightarrow{r_B}$ are defined as the z and x directions of the molecular coordinate system, respectively. Thus, the bent molecule considered in this has a biaxial shape with a direction normal to the molecular plane, defined as the y direction of the molecular coordinate system. As the intermolecular potential for the biaxial molecules, particularly, the potential for interacting via dispersion forces was introduced in a previous work [1], the terms in Eq. (10) can be written as follows:

$$\Phi(\vec{p}_A(I), \vec{p}_A(J)) = \Phi_r(|\vec{R}_{IJ} + \vec{r}_A(J) - \vec{r}_A(I)|)\left(sin\left(\frac{\theta_B}{2}\right)\right)^4 f(\varepsilon_x)\,, \tag{11}$$

$$\Phi\left(\vec{p}_A(I), \vec{p}_B(J)\right) = \Phi_r\left(\left|\vec{R}_{IJ} + \vec{r}_B(J) - \vec{r}_A(I)\right|\right)\left(sin\left(\frac{\theta_B}{2}\right)\right)^4 f(\varepsilon_x), \quad (12)$$

$$\Phi\left(\vec{p}_B(I), \vec{p}_A(J)\right) = \Phi_r\left(\left|\vec{R}_{IJ} + \vec{r}_A(J) - \vec{r}_B(I)\right|\right)\left(sin\left(\frac{\theta_B}{2}\right)\right)^4 f(\varepsilon_x), \quad (13)$$

$$\Phi\left(\vec{p}_B(I), \vec{p}_B(J)\right) = \Phi_r\left(\left|\vec{R}_{IJ}\right| + \vec{r}_B(J) - \vec{r}_B(I)\right)\left(sin\left(\frac{\theta_B}{2}\right)\right)^4 f(\varepsilon_x), \quad (14)$$

where $\vec{R}_{IJ} \equiv \vec{R}_J - \vec{R}_I$, that is the vector connecting the center of the I- and J-th molecules; $\vec{r}_A$ and $\vec{r}_B$ are the vectors connecting the center of the molecule and positions of the induced dipole in the group on sides A and B, respectively; and $f(\varepsilon_x)$ is defined as

$$f(\varepsilon_x) = \sum_{\alpha,\beta=x,y,z} Q_{11}^{\alpha\beta}(I)\, Q_{11}^{\alpha\beta}(J) + \frac{(\varepsilon_x)^2}{2-(\varepsilon_x)^2} \sum_{\alpha,\beta=x,y,z} \left[Q_{11}^{\alpha\beta}(I) R^{\alpha\beta}(J) + Q_{11}^{\alpha\beta}(J) R^{\alpha\beta}(I)\right] + \left(\frac{(\varepsilon_x)^2}{2-(\varepsilon_x)^2}\right)^2 \sum_{\alpha,\beta=x,y,z} R^{\alpha\beta}(I) R^{\alpha\beta}(J), \quad (15)$$

where $Q_{11}^{\alpha\beta}(I)$ and $R^{\alpha\beta}(I)$ are defined as follows. First, the unit vector $\vec{a}_1(I)$ was defined to extend along the long molecular axis; the unit vector $\vec{a}_2(I)$ was defined to extend along the vector $\overrightarrow{r_A} + \overrightarrow{r_B}$; and $\vec{a}_3(I) = \vec{a}_1(I) \times \vec{a}_2(I)$ was established to be normal to the molecular plane. Table I presents the relationship between the directions of the orthogonal coordinate system (ξ,η,ζ) in the molecular frame and orthogonal coordinate system (x, y, z) of the laboratory frame with cosines between two coordinate systems shown in terms of the Eulerian angles $(\theta_I, \varphi_I, \psi_I)$ (Fig. 3). Second, according to Priest and Lubensky [11], the tensors in Eq. (15) are defined as

$$Q_{pq}^{ij}(I) = a_p^i(I) a_q^j(I) - \frac{\delta_{pq}\,\delta_{ij}}{3} \text{ (p, q = 1,2,3; i, j = x,y,z)} \quad (16)$$

$$R^{\alpha\beta}(I) \equiv Q_{22}^{\alpha\beta}(I) - Q_{33}^{\alpha\beta}(I). \quad (17)$$

In Eq. (16), $a_p^i(I)$ denotes the i-th orthogonal component of unit vector $\vec{a}_p(I)$ parallel to the p-th principal axis of the I-th molecule, andδpq and δij are the Kronecker's delta functions. $\Phi_{IJ}\left(R_{IJ}\right)$ in Eq. (10) can be written as

$$\Phi_{IJ}\left(R_{IJ}\right) = 4\left(sin\left(\frac{\theta_B}{2}\right)\right)^4 \Phi_r\left(\left|\vec{R}_{IJ}\right|\right) f(\varepsilon_x). \quad (18)$$

The terms $\vec{r}_A(J) - \vec{r}_A(I)$, $\vec{r}_B(J) - \vec{r}_A(I)$, $\vec{r}_A(J) - \vec{r}_B(I)$, and $\vec{r}_B(J) - \vec{r}_B(I)$ in Eqs. (11—14) are neglected because they do not affect the orientational ordering in the nematic phase. However, they are considered to affect the translational ordering in the smectic phase, causing the smectic A-to-smectic C phase transition. This problem is discussed in detail in Section 5. The

interaction potential of the bent molecule interacting via dispersion forces is the same as that of the biaxial molecule investigated in previous studies by the same author.

FREE ENERGY AND PHASE DIAGRAM OF THE SYSTEM

The free energy of the model is expressed by the orientational orderings:

$$\sigma_1 = \langle \frac{3}{2} cos^2\theta_I - \frac{1}{2} \rangle_0 , \tag{19}$$

$$\sigma_2 = \langle sin^2\theta_I cos2\varphi_I \rangle_0 , \tag{20}$$

$$\sigma_3 = \langle \frac{3}{2} sin^2\theta_I cos2\psi_I \rangle_0 , \tag{21}$$

$$\sigma_4 = \langle \frac{1}{4} (cos^2\theta_I + cos^4\theta_I) cos2\varphi_I cos2\psi_I \rangle_0 . \tag{22}$$

where the angular brackets with the suffix zero denote that the average determined at thermal equilibrium. The total free energy of the system is written as

$$\begin{gathered} F(\{\sigma_1, \sigma_2, \sigma_3, \sigma_4\}; \varepsilon_x) = S_1(\sigma_1) + S_2(\sigma_{1,}\sigma_2) + S_3(\sigma_1, \sigma_3) + S_4(\sigma_1, \sigma_4) \\ -\frac{\beta}{2} 4 \left(sin \frac{\theta_B}{2} \right)^4 \bar{\Phi} \left\{ \left(\frac{2}{3} (\sigma_1)^2 + \frac{1}{2} (\sigma_2)^2 \right) + \frac{(\varepsilon_x)^2}{2 - (\varepsilon_x)^2} \left(\frac{4}{3} \sigma_1 \sigma_3 + 4\sigma_2 \sigma_4 + \frac{(\sigma_2)^2 \sigma_3}{1 - \sigma_1} \right) \right\} \\ -\frac{\beta}{2} 4 \left(sin \frac{\theta_B}{2} \right)^4 \bar{\Phi} \left(\frac{(\varepsilon_x)^2}{2 - (\varepsilon_x)^2} \right)^2 \left\{ \frac{2}{3} (\sigma_3)^2 + 8 (\sigma_4 + \frac{1}{4} \frac{\sigma_2 \sigma_3}{1 - \sigma_1})^2 \right\}, \end{gathered} \tag{23}$$

where interaction potential $\bar{\Phi}$ is defined as

$$\bar{\Phi} = \frac{4\pi}{3} \rho \int \Phi_r(r) r^2 dr . \tag{24}$$

where ρ is the average density of molecules in the system. We define the entropy terms in Eq. (23) as

$$S_1(\sigma_1) = \frac{1}{3} \{ (1 + 2\sigma_1) ln(1 + 2\sigma_1) + 2(1 - \sigma_1) ln(1 - \sigma_1) \}, \tag{25}$$

$$\begin{gathered} S_2(\sigma_{1,}\sigma_2) = \frac{1}{3} \left(1 - \sigma_1 + \frac{2}{3} \sigma_2 \right) ln \left(1 - \sigma_1 + \frac{2}{3} \sigma_2 \right) \\ + \frac{1}{3} \left(1 - \sigma_1 - \frac{2}{3} \sigma_2 \right) ln \left(1 - \sigma_1 - \frac{2}{3} \sigma_2 \right) - \frac{2}{3} (1 - \sigma_1) ln(1 - \sigma_1), \end{gathered} \tag{26}$$

$$\begin{gathered} S_3(\sigma_{1,}\sigma_3) = \frac{1}{3} (1 - \sigma_1 + \sigma_3) ln(1 - \sigma_1 + \sigma_3) \\ + \frac{1}{3} (1 - \sigma_1 - \sigma_3) ln(1 - \sigma_1 - \sigma_3) - \frac{2}{3} (1 - \sigma_1) ln(1 - \sigma_1), \end{gathered} \tag{27}$$

$$S_4(\sigma_1,\sigma_4) = \frac{1}{6}(1+2\sigma_1+6\sigma_4)ln(1+2\sigma_1+6\sigma_4)$$
$$+\frac{1}{6}(1+2\sigma_1-6\sigma_4)ln(1+2\sigma_1-6\sigma_4)-\frac{1}{3}(1+2\sigma_1)ln(1+2\sigma_1). \quad (28)$$

The symmetry-breaking potential method was applied to obtain the free energy of the system [Eq. (23)] by mechanically calculating the thermal average of the intermolecular potential [Eq. (18)] [12, 13]. The detailed the calculation was procedure was previously reported [1]. The free energy in Eq. (23) is minimized by determining the equilibrium with respect to the order parameters σs using the conditions:

$$\frac{\partial}{\partial\sigma_s}F(\{\sigma_1,\sigma_2,\sigma_3,\sigma_4\};\varepsilon_x) = 0 \text{ (S = 1, 2, 3, 4).} \quad (29)$$

In Eq. (23), temperature T is normalized as

$$\tilde{T} \equiv k_BT/4\left(sin\frac{\theta_B}{2}\right)^4\bar{\Phi} = (1+(\varepsilon_x)^2)^2\frac{k_BT}{4\bar{\Phi}} = (1+(\varepsilon_x)^2)^2\frac{\overline{U^0_{dis}}}{2\bar{\Phi}}\bar{T}. \quad (30)$$

The phase diagram of the normalized temperature $\tilde{T}$ versus ε_x was previously constructed in Ref. [1], as shown in Fig. 4(a). The transition sequence in $0 \leq \varepsilon_x \leq 1$ of the previous model has seven phase transitions patterns [1], whereas that of the proposed model has only four patterns because ε_x is limited from 0 to $\sqrt{3}/3 \approx 0.5774$.

Moreover, T is normalized with $4\bar{\Phi}/k_B$ and $1/(1+(\varepsilon_x)^2)^2$. However, the dependence of the normalized temperature $\tilde{T}$ on ε_x is not sufficient to change the dependence of the temperature $\bar{T}$ on ε_x. Overall, three transition sequences may have existed in the present model. As the temperature increases from 0, the following phase transitions occur: (1) phase biaxial nematic (NPB) phase → molecular biaxial nematic (NMB) phase → uniaxial nematic (N) phase → isotropic (Iso) phase when $\varepsilon_x^0 \leqq 0.155$, (2) NPB phase → NMB phase → N phase → NMB phase → Iso phase when $0.155 \leqq \varepsilon_x^0 \leqq 0.165$, and (3) NPB phase → NMB phase → Iso phase when $0.165 \leqq \varepsilon_x^0 \leqq 0.5774$. [Fig. 4(b)]. The notation "A → B" indicates that phase B exists at a higher temperature than phase A.

CONCLUSIONS

A system of molecules with bent cores demonstrated sequence of phase transitions between various nematic and isotropic phases. This study proposed a theory, whereby the θ_B and ε_x values and sequence of phase transitions depend on the ratio of the strength of two intramolecular forces that impose at limitation on θ_B, which was denoted as u. Furthermore, the intramolecular forces governed the phase transitions between various nematic phases.

In the assembly of target molecules, the SmA, and SmC were found besides nematic phase [14]. However, in present study, only the orientational order parameters are considered in constructing molecular theory of phase transitions in the assembly of molecules with a bent core interacting via dispersion forces. So then, the results of present study can't elucidate the existence of smectic phases in the assembly of target molecules. However, if not only the orientational order parameters but also the translational one is considered in present model,

such a study is able to elucidate perfectly phase transitions including smectic phase in the assembly of target molecule. The investigations of phase transitions including smectic phase in the assembly of various molecules were carried out by present author and many results relating to phase transitions including smectic phase were obtained. [15 − 19]

In this study, the terms $r_A^{\rightarrow}$ (J)- $r_A^{\rightarrow}$ (I), $r_B^{\rightarrow}$ (J)- $r_A^{\rightarrow}$ (I), $r_A^{\rightarrow}$ (J)- $r_B^{\rightarrow}$ (I), and $r_B^{\rightarrow}$ (J)- $r_B^{\rightarrow}$ (I) were neglected, because they do not affect the orientational ordering. However, an investigation of the factors that influence the smectic phase revealed that these terms contribute to the translational ordering; thus, these terms should be included to clarify the transitions involving the smectic phase, particularly the smectic A-to-C phase transition.

Approximately 40 years ago, van der Meer and Vertogen [20] proposed a molecular model to investigate the smectic A-to-C phase transition based on the permanent dipole of a molecule and the induced dipole of the molecule interacting with each other. This study obtained a similar theory that can explain the smectic A-to-C phase transition. The author endeavors to further investigate this problem in future studies.

The theory presented here is also applicable to the molecular model of dimers linked by a flexible chain. However, this theory considered the internal rotation between gauche and trans conformations of the C — C bond in the alkyl chain, which are more complicated than that presented in this study. However, as this internal rotation results in the chiral shape of molecule, the proposed theory can be applied to investigate the smectic C and smectic C* (chiral smectic C) phase transition. Therefore, the presented theory for bent liquid crystals is applicable for investigating smectic A, C, and C* phases.

Generally, a bent liquid crystal molecule has a permanent electric dipole, including the ordering of permanent dipoles in the system and consequently, including the various phases that cannot appear without the ordering of these electric dipole, resulting in the ferro-electric effect of molecule. Thus, the permanent electric dipole is important for the phase transition of the system of bent molecule; However, this was not considered in this study because the orientational orderings in the system of biaxial molecules was not considered to be induced by the interaction between each permanent electric dipole of the molecules but by the dispersive interaction between each biaxial molecule. In this study, only orientational transitions in a system of bent molecules were investigated; thus, only their dispersive interaction was introduced. In our future works, the theory of a system of bent molecules with consideration of the permanent electric dipole and their phase transitions will be investigated.

Acknowledgments
I would like to thank Editage (www.editage.jp) for their English language editing services.

Disclosure Statements
No potential conflict of interest is reported by the author.

References
[1] M. Hosino, & H. Nakano, *Mol. Cryst. Liq. Cryst.* 348(1), 207—225(2000).

[2] M. Hosino, *Mol. Cryst. Liq. Cryst.* 658(1), 1－12(2017).

[3] M. Hosino, *Mol. Cryst. Liq. Cryst*. 658(1), 92－107(2017).

[4] M. Hosino, & K. Ijuin, *SCIREA J. Chem.* 6, 21－47(2021).

[5] M. Hosino, *Mol. Cryst. Liq. Cryst*. 768(1), 108－118(2023).

[6] H. Takezoe, & A. Eremin, *Bent-shaped Liquid Crystals*, *Chapter 1*, (CRC Press, Boca Raton, 2017), pp. 1－10.

[7] A. Matsuyama, *Mol. Cryst. Liq. Cryst.* 714 1－9(2021).

[8] K. Miyagi, & A. Matsuyama, *Mol. Cryst. Liq. Cryst.* 757 13－21(2023).

[9] A. G. Vanakaras, & D. J. Photinos, *Soft. Matter* 12(7), 2208－2220(2016).

[10] A. Matsuyama, *Liq. Cryst.* 46(15), 2301－2321(2019).

[11] R.G. Priest, & T.C. Lubensky, *Phys. Rev.* A9, 893－898(1974).

[12] H. Nakano, & M. Hattori, *Prog. Theor. Phys* 49, 1752－1754(1973).

[13] H. Nakano, & H. Kimura, *Statistical Thermodynamics of Phase Transitions (in Japanese)*, *Chapter 3*, (Asakura, Tokyo, Japan, 1988), pp. 41—78.

[14] A. Eremin, H. Nadashi, G. Pelzl, S. Diele, H. Kresse, W. Weissflog, & S. Grande, *Phys. Chem. Chem. Phys. 6*, 1290—1298(2004).

[15] M. Hosino, H. Nakano, & H. Kimura, *J. Phys. Soc. Jpn.* 46(6), 1709－1715(1979).

[16] M. Hosino, H. Nakano, & H. Kimura, *J. Phys. Soc. Jpn.* 47(3), 740－745(1979).

[17] M. Hosino, H. Nakano, & H. Kimura, *J. Phys. Soc. Jpn.* 50(4), 1067－1072(1981).

[18] M. Hosino, H. Nakano, & H. Kimura, *J. Phys. Soc. Jpn.* 51(3), 741－748(1982).

[19] M. Hosino, & H. Nakano, *J. Phys. Soc. Jpn.* 65(4), 978－983(1996).

[20] B.W. Van der Meer, & G. Vertogen, *J. Phys. (Paris)* 40, C3-222. ― C3-228(1979).

TABLES AND FIGURES

Table I: Direction cosines between the molecular and laboratory frames

	x	y	z
ξ	*cosθ cosφ cosψ- sinφ sinψ*	*cosθ sinφ cosψ+ cosφ sinψ*	*-sinθ cosψ*
η	*-cosθ cosφ sinψ- sinφ cosψ*	*-cosθ sinφ sinψ+ cosφ cosψ*	*sinθ sinψ*
ζ	*sinθ cosφ*	*sinθ sinφ*	*cosθ*

(ξ,η,ζ): coordinate axes in the molecular reference frame.
(x, y, z): coordinate axes in the laboratory reference frame.

Table II: Seven patterns of transition sequences

	Phase transition sequence	ε_x range
1	$I \rightarrow N$	$\varepsilon_x = 0$
2	$I \rightarrow N \rightarrow N_{MB} \rightarrow N_{PB}$	$0 \leqq \varepsilon_x \leqq 0.115$
3	$I \rightarrow N_{MB} \rightarrow N \rightarrow RN_{MB} \rightarrow N_{PB}$	$0.115 \leqq \varepsilon_x \leqq 0.165$
4	$I \rightarrow N_{MB} \rightarrow N_{PB}$	$0.165 \leqq \varepsilon_x \leqq 0.705$
5	$I \rightarrow N_{PB}$	$\varepsilon_x = 0.705$
6	$I \rightarrow D_N \rightarrow N_{PB}$	$0.705 \leqq \varepsilon_x \leqq 1$
7	$I \rightarrow D_N$	$\varepsilon_x = 1$

"A→B" indicates that phase B appears after phase A as the temperature decreases. RNMB in pattern3 indicates that the molecular biaxial phase appeared at temperatures lower than those at which the N phase appeared, denoting the re-emergence of the NMB phase.

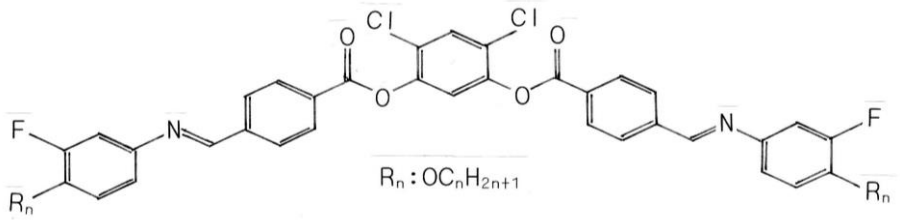

Figure 1(a). Chemical structure of compound analyzed in this study.

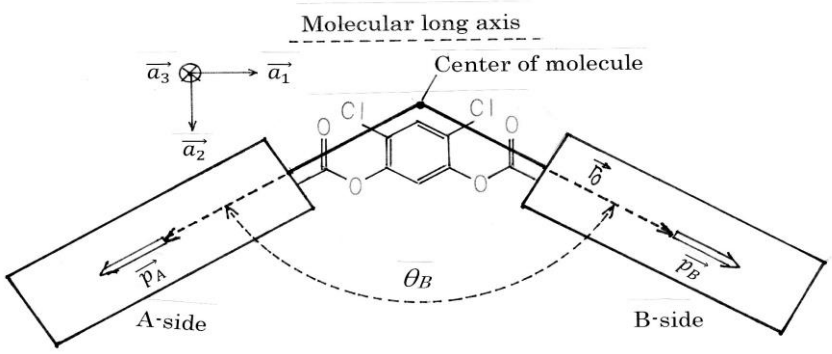

Figure 1(b). Schematic of the molecule and its parameters.

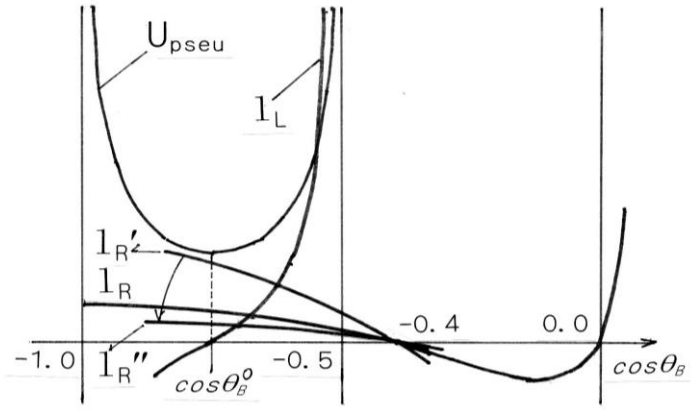

Figure 2(a). Graphical solusion of Eq. (6) for the case of u = 1.0. In this case, $cos\theta_B^0$ = − 0.75, and Upseu is drawn as its magnitudes are multiplied by 10 with the magnitudes of lL, lR, lR′, and lR″. lR is the line at which the normalized temperature $\overline{T}$ = 1. lR changes from lR′, to lR, and finally lR″ as the temperature increases. Thus, $cos\theta_B$ asymptotically approaches $cos\theta_B^0$.

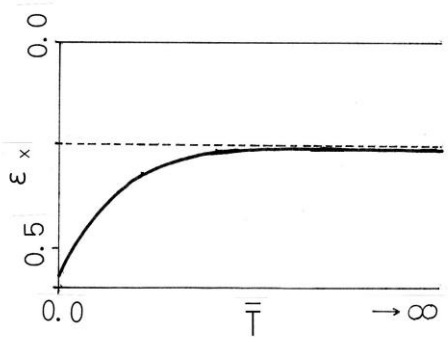

Figure 2(b). Dependence of anisotropic parameter εx on temperature; ε_x= 0.5774 when the temperature is zero and decreases asymptotically to ε_x^0 as the temperature increases to infinity.

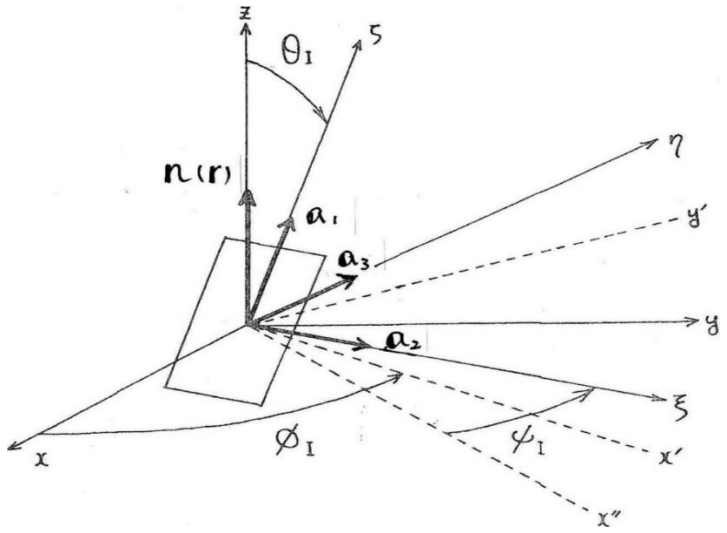

Figure 3. Eulerian angles (θI, φI, ψI) showing the direction cosines between the orthogonal coordinate system in the molecular and laboratory frames (TableI)

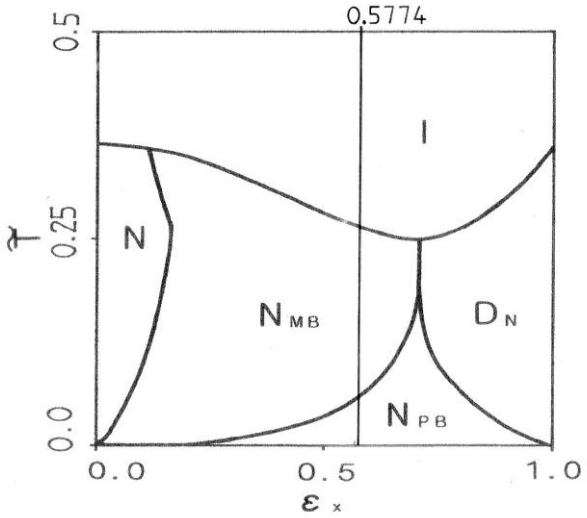

Figure 4(a). Phase diagram on the plane of the temperature versus the anisotropy parameter, ε_x. As θ_B is limited to the range of $2\pi/3$ and π, εx is limited from 0 ($\theta_B = \pi$) to $\sqrt{3}/3 \approx 0.5774$ ($\theta_B = 2\pi/3$). This figure is based on the work in Hosino & Nakano [1] with the addition of $\varepsilon x = \sqrt{3}/3 \approx 0.5774$.

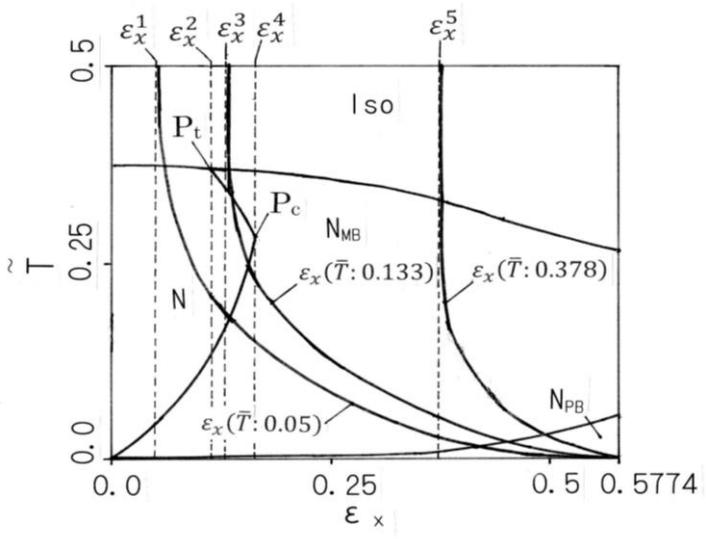

Figure 4(b). Values of the anisotropic parameters: ε_x^1, ε_x^2, ε_x^3, ε_x^4, and ε_x^5 are 0.05, 0.115, 0.133, 0.165, and 0.378, respectively. ε_x^2 and ε_x^4 are the εx values at points Pt and Pc, respectively. εx becomes ε_x^5 when u is unity. When $\theta_B = 168^\circ$, which is the maximum experimental value [10], εx becomes ε_x^3.